

Fast Event-based Optical Flow Estimation by Triplet Matching

Shintaro Shiba^{1,2}, Yoshimitsu Aoki¹, Guillermo Gallego^{2,3}

Abstract—Event cameras are novel bio-inspired sensors that offer advantages over traditional cameras (low latency, high dynamic range, low power, etc.). Optical flow estimation methods that work on packets of events trade off speed for accuracy, while event-by-event (incremental) methods have strong assumptions and have not been tested on common benchmarks that quantify progress in the field. Towards applications on resource-constrained devices, it is important to develop optical flow algorithms that are fast, light-weight and accurate. This work leverages insights from neuroscience, and proposes a novel optical flow estimation scheme based on triplet matching. The experiments on publicly available benchmarks demonstrate its capability to handle complex scenes with comparable results as prior packet-based algorithms. In addition, the proposed method achieves the fastest execution time (> 10 kHz) on standard CPUs as it requires only three events in estimation. We hope that our research opens the door to real-time, incremental motion estimation methods and applications in real-world scenarios.

Index Terms—Event cameras, optical flow, low latency, asynchronous sensor, neuroscience, robotics.

I. INTRODUCTION

EVENT cameras [1], [2] have led to rethinking visual processing for various computer vision tasks because their operating principle and output data are fundamentally different from those of conventional, frame-based cameras. These bio-inspired sensors naturally respond to the scene dynamics and offer advantages, such as low latency, high dynamic range (HDR) and data efficiency, which need to be unlocked with new algorithms [3]. Neuromorphic principles have been a major source of inspiration for such novel algorithms and hardware, especially in motion estimation tasks [4]–[6].

Event-based optical flow estimation methods can be broadly classified as *packet-based* or *event-by-event*-based depending on how events are processed and update the estimator’s output. Packet-based methods process a batch of events (e.g., events in a fixed time window, say 10–100 ms, or a fixed number of events, typically 30k–1M), hence they require some waiting time before processing (inference) starts [7]–[10]. They trade off the high-speed advantages of event data for accuracy. Prior work has proposed adaptations of classical frame-based methods (block matching [10], Lucas-Kanade [11]), spatio-temporal plane-fitting [8], [12], time-surface matching [13], and contrast-maximization methods [7], [9], [14]. While the above methods are model-based (optimization) methods, Artificial Neural Networks (ANN) [15]–[19] are also batch-based,

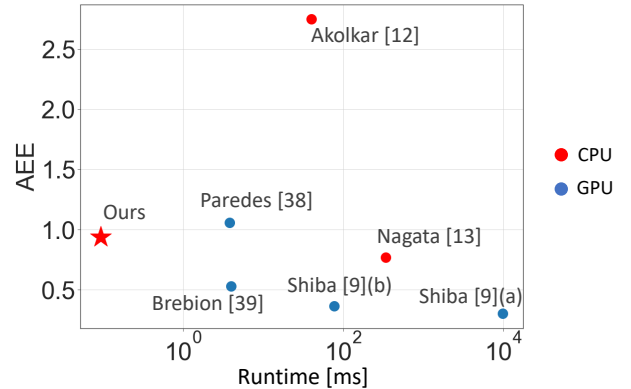


Fig. 1: *Runtime vs. accuracy comparison* for various event-based optical flow estimation methods. Results are on outdoor data of the MVSEC benchmark [15] (see also Tab. II). Accuracy is measured based on Average Endpoint Error (AEE). Shiba [9](a) and Shiba [9](b) denote optimization-based and DNN-based results, respectively.

and are inspired by frame-based ANN architectures [20], [21], thus requiring data conversion into a tensor representation, such as voxel grids. ANNs achieve current state-of-the-art accuracy for optical flow estimation and high speed [9], [17], but require power-hungry GPUs and lack interpretability.

On the other hand, event-by-event methods process every event incrementally as it occurs (without waiting time), aiming to leverage the camera’s low-latency advantage [5], [22]. Many event-by-event methods, such as Spiking Neural Networks (SNNs), are inspired by the brain (i.e., *neuromorphic*), since the neural circuits of visual processing are thought to be event-driven. While previous work propose SNN architectures [6], [23], [24], they comprise low-level physiological parameters of neurons (e.g., membrane potentials) that are difficult to interpret, validate and adjust to improve the estimation accuracy. Indeed, insects and mammals have different low-level underlying mechanisms, while they have similar algorithmic steps to transform light into motion [25]. Hence, it is important to find abstracted logical operations of motion estimation, rather than to mimic the entire physiological properties of neurons. From a practical point of view, most event-by-event methods have been tested on simple scenes, as opposed to the more complex real-world scenes and publicly-available benchmarks of batch-based methods [26]. This may be attributed to the use of tailored hardware [4], strong assumptions of the scene, limited problem settings [5] or the difficulty in defining event-by-event benchmarks on real data with μ s resolution. Hence,

¹ Department of Electronics and Electrical Engineering, Faculty of Science and Technology, Keio University, Kanagawa, Japan. ² Department of Electrical Engineering and Computer Science, Technische Universität Berlin, Berlin, Germany. ³ Einstein Center Digital Future and Science of Intelligence Excellence Cluster, Berlin, Germany.

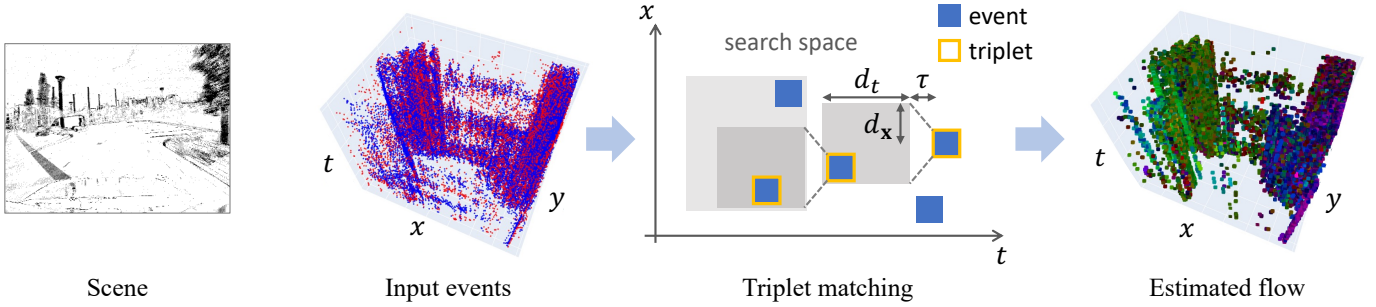


Fig. 2: *Triplet matching algorithm*. The algorithm seeks spatially and temporally neighboring events in an event-by-event manner, and provides event-based flow \mathbf{f}_k . For ease of visualization we only show the search in x and t , but it is actually carried out in x, y and t . Note this is an example of batch estimation given the input events.

it is important to explore event-by-event motion estimation algorithms that can solve complex, real-world problems.

This work leverages insights from neuroscience, especially from the classical Barlow-Levick model [27], and proposes a novel optical flow estimation scheme based on correlation of occurrence. In contrast to previous batch-based methods, it requires only three events (triplet) for estimation, which opens the door to future real-time incremental motion estimation methods. Compared to previous event-by-event approaches, it is tested on publicly-available optical flow benchmarks to demonstrate its capability to handle real-world scenes with comparable results. Additionally, it is based on logical operations, which enables a simple and efficient data structure implementation and execution on standard CPUs. In summary, our contributions are twofold: (i) we present a novel event-by-event algorithm for optical flow estimation, theoretically derived from neuroscience insights, and (ii) we practically demonstrate that it achieves comparable results as prior work while only requiring a CPU and being faster than optimization-based algorithms (Fig. 1).

The signal processing in this work materializes the ideas in current neuroscience models, shedding light on what the strong and weak scenarios are, in order to improve the models.

II. METHODOLOGY

A. Event Camera

Event cameras acquire visual data in the form of asynchronous per-pixel brightness differences called “events” [1], [3]. An event $e_k \doteq (t_k, \mathbf{x}_k, p_k)$ is triggered as soon as the logarithmic brightness at the pixel $\mathbf{x}_k \doteq (x_k, y_k)^\top$ exceeds a preset threshold. Here, t_k is the timestamp of the event with μs resolution, and polarity $p_k \in \{+1, -1\}$ is the sign of the brightness change (i.e., increase vs. decrease, respectively).

B. Triplet Matching

The idea of the triplet matching comes from neuroscience models by Hassenstein-Reichardt [28] and Barlow-Levick [27]. These correlator models estimate motion by computing pairwise neural activities (e.g., spikes) in space and time [25]. Especially, [29] suggests that triplet correlations (the product of pairwise correlations for three spikes in space-time) improve

Algorithm 1 Triplet matching algorithm

Input: e_k, \mathcal{H}^{k-1}

Output: $\mathcal{H}^k, \mathbf{f}_k$

- 1: Find event neighborhood H_k in (1).
 - 2: **for** $i \in H_k$ **do**
 - 3: Search for triplet candidates (2).
 - 4: Collect triplet $T = (k, i, j)$
 - 5: **end for**
 - 6: Calculate $\mathbf{f}_k \leftarrow \{T\}$ in (3)
 - 7: Update $\mathcal{H}^k \leftarrow \mathcal{H}^{k-1}, H_k$
-

motion estimation accuracy. Here, we introduce the idea of the triplet-matching method as logical operations in space-time coordinates. We build an incremental (event-by-event) estimation algorithm, and extend it into batch mode for testing because benchmarks are specified on a batch basis.

1) *Incremental Estimation*: It consists of two main steps: *search* and *update* (Algorithm 1). Events are split by polarity, following the idea of ON- and OFF- circuits in the brain [25]. The search step finds triplets of events that are aligned (i.e., correlated) in space-time assuming a constant velocity model (Fig. 2). One of the events in the triplet is the incoming event, and the other two events are searched for within its space-time neighborhoods of size d_x, d_t . The search has two steps: first the set of all potential 2nd events is determined; then the set of all potential 3rd events (compatible with the previous two in the triplet) refines the search. In the update step, every triplet of events is characterized by a different velocity. The velocity (flow) \mathbf{f}_k for the incoming event e_k is computed as the average of the velocities of all triplets. Later, for benchmarking purposes, the flow is voxelized (quantized on a space-time grid) and smoothed.

In the *search step*, since event data are sorted by timestamp t , we use index maps to make the search efficient, with complexity $O(N_e \log N_e)$. The index map H_k of an event e_k consists of the indices of its space-time neighbors:

$$H_k = \{i \mid t_k - \tau - d_t \leq t_i \leq t_k - \tau \text{ and } \|\mathbf{x}_k - \mathbf{x}_i\| \leq d_x\}. \quad (1)$$

Parameters d_t and d_x decide the maximum admissible velocity of the flow, and τ is a *refractory period*, which limits the search space by assuming neighboring events in the moving

edge do not exist at the same timestamp. d_t can also be interpreted as the *delay* in the Barlow-Levick model. For each new event e_k , we build a set of index maps $\mathcal{H}^k = \{H_i\}_{i=1}^k$ and output a set of event triplets $\{T\} \doteq \{(e_k, e_i, e_j)\}$. To find the triplet match we look for event indices j that have roughly constant velocity with the event pairs (e_k, e_i) where $i \in H_k$:

$$J_{k,i} = \{j \in H_i \mid t_i - \tau - d_t \leq t_j \leq t_i - \tau \text{ and } \mathbf{x}_i - \mathbf{x}_j = \mathbf{x}_k - \mathbf{x}_i\}. \quad (2)$$

The *update step* calculates the flow \mathbf{f}_k and updates the index map \mathcal{H}^k . \mathcal{H}^k is obtained by adding new H_k to \mathcal{H}^{k-1} and removing old index maps (we keep the last 20000 index maps per polarity). The flow \mathbf{f}_k is obtained as the weighted average

$$\mathbf{f}_k \doteq \frac{\sum_T w_T \mathbf{v}_T}{\sum_T w_T}, \quad (3)$$

where $\mathbf{v}_T \doteq (\mathbf{x}_j - \mathbf{x}_k)/(t_j - t_k)$ is the velocity of each triplet. Since (3) gives accurate flow if the triplet is caused by the same scene edge, we use the weight w_T to estimate the probability that the triplet belongs to the same edge. Assuming constant velocity, if e_j is produced by the same edge that generates e_k and e_i , the expected timestamp of e_j is given by $\hat{t}_j = t_i - \delta$, where $\delta \doteq t_k - t_i$. Therefore, to account for errors in the timestamps between \hat{t}_j and t_j , we set the weight $w_T \doteq \mathcal{N}(t_j; \hat{t}_j, \delta^2)$, where \mathcal{N} is the Gaussian density function. The proposed average flow due to the triplets (3) may not necessarily equal the optical flow but this strong assumption is justified by the empirical results (Sec. III).

2) *Batch Estimation*: We extend the incremental (event-by-event) estimator to batch mode because current benchmarks are batch-based. For a set of events $\mathcal{E} \doteq \{e_k\}_{k=1}^{N_e}$, we create the index maps \mathcal{H}^{N_e} first, which takes $O(N_e^2 \log N_e)$. Then the flow is calculated looping over each event using Algorithm 1. The overall computational complexity is $O(N_e^2 \log N_e)$.

For benchmarking with ground truth, the event-wise flow is converted into a voxel-wise flow, which also enhances space-time coherence. We quantize the time coordinates of \mathbf{f}_k into bins, and take the average of the $\{\mathbf{f}_k\}$ that lie in each voxel. We also apply a non-zero average filter (take average of only non-zero values) with kernel size 3×3 for spatial smoothing.

The computational complexity of both approaches is summarized in Tab. I. For comparison, we also report those of state-of-the-art methods: Contrast Maximization (CMax) approaches [7], [9] and time-surface matching [13]. The latter methods require additional complexity for the number of iterations N_{iter} . We report runtime comparisons in Sec. III-C.

TABLE I: Complexity of algorithms, for batch estimation and event-by-event estimation.

	Batch	Event-by-event
CMax [7]	$O(N_{\text{iter}}(N_e + N_p))$	–
Nagata et al. [13]	$O(N_{\text{iter}}(N_e + N_p))$	–
Ours	$O(N_e^2 \log N_e)$	$O(N_e \log N_e)$

III. EXPERIMENTS

A. Datasets and Evaluation Metrics

The MVSEC dataset [30] is a standard dataset for optical flow estimation [6], [9], [16], [17]. The data consists of

TABLE II: Results on MVSEC dataset [15]. Methods are presented as unsupervised learning-based (USL) or model-based (MB). For brevity, EV-FlowNet is abbreviated as EVFN. Nagata et al. [13] evaluate on shorter time intervals; for comparison, we scale the errors to $\Delta t = 1$.

	$\Delta t = 1$	outdoor_day1		indoor_flying1		indoor_flying2	
		AEE ↓	%Out ↓	AEE ↓	%Out ↓	AEE ↓	%Out ↓
USL	EVFN [16]	0.3	0.0	0.6	0.0	1.0	4.0
	EVFN (retrain) [38]	0.9	5.4	0.8	1.2	1.4	10.9
	FireFlowNet [38]	1.1	6.6	1.0	2.6	1.7	15.3
	ConvGRU-EVFN [6]	0.5	0.3	0.6	0.5	1.2	8.1
	MultiCM-EVFN [9]	0.4	0.1	–	–	–	–
MB	Nagata et al. [13]	0.8	–	0.6	–	0.9	–
	Akolkar et al. [12]	2.8	–	1.5	–	1.6	–
	Brebion et al. [39]	0.5	0.2	0.5	0.1	1.0	5.5
	MultiCM [9]	0.3	0.1	0.4	0.1	0.6	0.6
	Ours	0.9	3.1	1.1	2.9	1.7	13.4

		$\Delta t = 4$					
		outdoor_day1		indoor_flying1		indoor_flying2	
		AEE ↓	%Out ↓	AEE ↓	%Out ↓	AEE ↓	%Out ↓
USL	EVFN [16]	1.3	9.7	2.2	24.2	3.9	46.8
	ConvGRU-EVFN [6]	1.7	12.5	2.2	21.5	3.9	40.7
	MultiCM-EVFN [9]	1.5	11.7	–	–	–	–
MB	MultiCM [9]	1.2	9.2	1.7	12.9	2.5	26.3
	Ours	3.6	49.0	4.1	53.9	6.4	71.8

event camera, LiDAR, and camera poses. The event camera (mDAVIS346 camera [31]) provides events, grayscale frames and IMU data (346×260 pix). The ground truth optical flow is provided as the motion field from the camera velocity and the depth of the scene [15]. The sequences are indoors with a drone and outdoors with a car, and we evaluate on 63.5 million events spanning 265 seconds from both outdoor and indoor sequences.

We measure optical flow accuracy to evaluate our method. The metrics are the Average Endpoint Error (AEE) and the percentage of pixels with AEE greater than 3 pixels (% Out). The time intervals for evaluation are $\Delta t = 1$ grayscale frame (at ≈ 45 Hz, i.e., 22.2ms) and $\Delta t = 4$ frames (89ms). Flow accuracy is evaluated only in pixels with valid ground truth. All experiments use $d_x = \sqrt{2}$ pix, $d_t = 100$ ms and $\tau = 3$ ms.

We also show additional results on the ECD dataset [32], which is widely used for motion estimation [33]–[36]. Each sequence provides events, frames, calibration, and IMU data (at 1 kHz) from a DAVIS240C (240×180 pix) [37], as well as ground truth camera poses (at 0.2 kHz).

B. Optical Flow Estimation Accuracy

Table II comprises flow estimation accuracy results on the MVSEC benchmark. The top part of the table reports results for $\Delta t = 1$, and the bottom part reports $\Delta t = 4$. The methods in the table are categorized as unsupervised learning-based (USL), i.e., using a Deep Neural Network (DNN) on grid-converted events, and model-based (MB). Results for $\Delta t = 1$ are thorough, with our method in the middle accuracy range among all methods. Results for $\Delta t = 4$ are not as complete because the literature does not report them (especially most model-based methods). While a thorough comparison for $\Delta t = 4$ is difficult, our error is roughly four times bigger

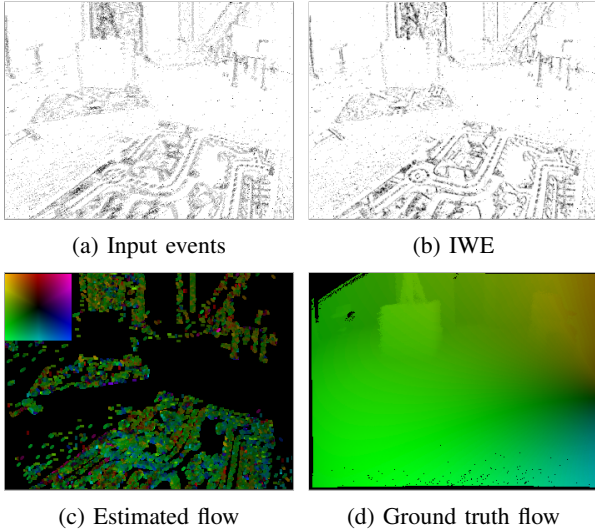


Fig. 3: Optical flow results on MVSEC data.

than for $\Delta t = 1$, which makes sense, and it is consistently 2.5–3 times bigger than that of the most accurate method [9] for both $\Delta t = \{1, 4\}$. The fact that for longer time intervals batch-based methods ($\Delta t = 4$) achieve higher accuracy than our method may be attributed to the fact that our method is event-by-event, so it does not leverage long-term temporal smoothing, which would improve robustness to noise.

The results in Fig. 3 show that the events displaced using the estimated flow produce sharp images of warped events (Fig. 3b, IWEs [7]). The Flow Warp Loss [40] measures the sharpness of the IWE: 1.154 for outdoor_day1, 1.157 for indoor_flying1, and 1.248 for indoor_flying2, where $\text{FWL} > 1$ indicates sharper than the identity warp baseline (i.e., zero flow). The figure also shows the estimated flow (Fig. 3c, and color wheel); notice that our method produces a flow vector for each event (Fig. 2), whereas it is common to display the flow for every pixel (image-based legacy). Hence, Fig. 3 shows a 2D collapsed version of the estimated space-time optical flow field, for visual comparison with the ground truth (Fig. 3d). The flow is most reliably estimated in regions where events happen, i.e., scene edges. Further spatial and temporal smoothness could be enhanced if needed: for example, homogeneous brightness regions between edges could be filled in by some prior, such as a regularizer or in-painting algorithm.

C. Runtime Comparison

The proposed method runs in an event-by-event manner, hence trades off accuracy for speed, compared with batch-based methods. We showed computational complexity comparison in Tab. I. Now, we conduct the runtime comparison among several previous work. We use Python (3.9.12) on CPUs (Mac M1 2020, 8 Cores) and average the runtime of processing 300k events incrementally. The results are shown in Fig. 1. Our method achieves the fastest runtime among compared methods: 0.0934 milliseconds (> 10 kHz). Note that many methods in the literature, such as the 2nd and 3rd fastest ones [38], [39], use GPUs, while ours runs natively on CPUs. This is crucial for applications on resource-constrained platforms.

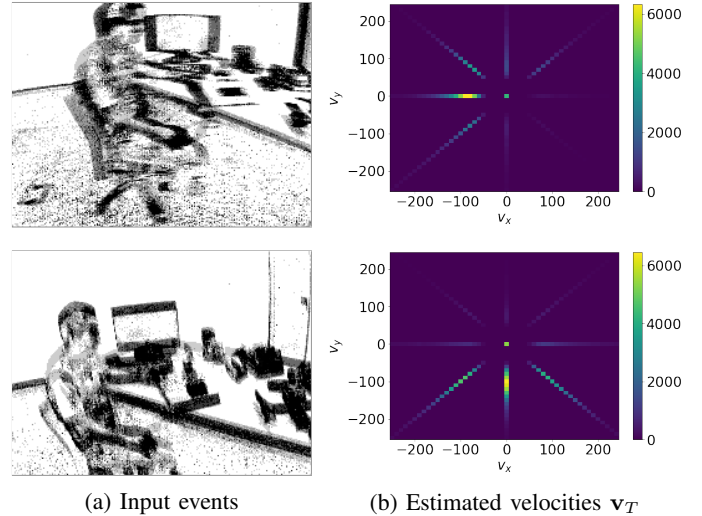


Fig. 4: Effect of pixel quantization on ECD data. In the top row the motion is dominantly horizontal, whereas in the bottom row it is vertical, as can be seen by the thickness of the edges (left) and the velocity distributions (right).

D. Effect of Pixel Quantization

A limitation of the proposed method is the quantization of the flow direction since the search for the second event in the triplet is limited to the 8 neighboring pixels of the current event. To illustrate it, we conduct experiments on the *dynamic_translation* sequence from the ECD dataset [32]. Figure 4 shows the distribution of \mathbf{v}_T over all events (assuming a planar translation model, i.e., constant velocity over all pixels). Similar to the SNN proposed in [23], \mathbf{v}_T is constrained to eight cardinal directions. However, in contrast to [23], which quantizes both the direction and magnitude of the flow, our method can estimate a continuum of magnitudes. The distributions are spread around a main direction and its two neighboring ones, which is due to the small aperture (5×5 pix) used for each triplet.

IV. CONCLUSION

We proposed a novel event-based optical flow estimation scheme based on triplet matching inspired by motion estimation models in neuroscience. The experiments demonstrate that it is considerably fast (> 10 kHz) on standard CPUs while providing comparable results as prior batch-based algorithms. We hope that our work opens the door to real-time, realistic, incremental motion estimation methods and event-camera applications on resource-constrained devices.

V. ACKNOWLEDGMENT

We thank Dr. R. Tanaka for useful discussions. This research was funded by the German Academic Exchange Service (DAAD), Research Grant-Bi-nationally Supervised Doctoral Degrees/Cotutelle, 2021/22 (57552338) and the Deutsche Forschungsgemeinschaft (DFG, German Research Foundation) under Germany’s Excellence Strategy – EXC 2002/1 “Science of Intelligence” – project number 390523135.

REFERENCES

- [1] P. Lichtsteiner, C. Posch, and T. Delbruck, "A 128×128 120 dB 15 μ s latency asynchronous temporal contrast vision sensor," *IEEE J. Solid-State Circuits*, vol. 43, no. 2, pp. 566–576, 2008.
- [2] T. Finateu, A. Niwa, D. Matolin, K. Tsuchimoto, A. Mascheroni, E. Reynaud, P. Mostafalu, F. Brady, L. Chotard, F. LeGoff, H. Takahashi, H. Wakabayashi, Y. Oike, and C. Posch, "A 1280×720 back-illuminated stacked temporal contrast event-based vision sensor with 4.86μ m pixels, 1.066Geps readout, programmable event-rate controller and compressive data-formatting pipeline," in *IEEE Intl. Solid-State Circuits Conf. (ISSCC)*, 2020, pp. 112–114.
- [3] G. Gallego, T. Delbruck, G. Orchard, C. Bartolozzi, B. Taba, A. Censi, S. Leutenegger, A. Davison, J. Conradt, K. Daniilidis, and D. Scaramuzza, "Event-based vision: A survey," *IEEE Trans. Pattern Anal. Mach. Intell.*, vol. 44, no. 1, pp. 154–180, 2022.
- [4] G. Haessig, A. Cassidy, R. Alvarez-Icaza, R. Benosman, and G. Orchard, "Spiking optical flow for event-based sensors using IBM's trueneurosynaptic system," *IEEE Trans. Biomed. Circuits Syst.*, vol. 12, no. 4, pp. 860–870, Aug. 2018.
- [5] T. Brosch, S. Tschechne, and H. Neumann, "On event-based optical flow detection," *Front. Neurosci.*, vol. 9, no. 137, Apr. 2015.
- [6] J. J. Hagenars, F. Paredes-Valles, and G. C. H. E. de Croon, "Self-supervised learning of event-based optical flow with spiking neural networks," in *Advances in Neural Information Processing Systems (NeurIPS)*, vol. 34, 2021, pp. 7167–7179.
- [7] G. Gallego, H. Rebecq, and D. Scaramuzza, "A unifying contrast maximization framework for event cameras, with applications to motion, depth, and optical flow estimation," in *IEEE Conf. Comput. Vis. Pattern Recog. (CVPR)*, 2018, pp. 3867–3876.
- [8] R. Benosman, C. Clercq, X. Lagorce, S.-H. Ieng, and C. Bartolozzi, "Event-based visual flow," *IEEE Trans. Neural Netw. Learn. Syst.*, vol. 25, no. 2, pp. 407–417, 2014.
- [9] S. Shiba, Y. Aoki, and G. Gallego, "Secrets of event-based optical flow," in *Eur. Conf. Comput. Vis. (ECCV)*, 2022.
- [10] M. Liu and T. Delbruck, "Adaptive time-slice block-matching optical flow algorithm for dynamic vision sensors," in *British Mach. Vis. Conf. (BMVC)*, 2018, pp. 1–12.
- [11] R. Benosman, S.-H. Ieng, C. Clercq, C. Bartolozzi, and M. Srinivasan, "Asynchronous frameless event-based optical flow," *Neural Netw.*, vol. 27, pp. 32–37, 2012.
- [12] H. Akolkar, S.-H. Ieng, and R. Benosman, "Real-time high speed motion prediction using fast aperture-robust event-driven visual flow," *IEEE Trans. Pattern Anal. Mach. Intell.*, vol. 44, no. 1, pp. 361–372, 2022.
- [13] J. Nagata, Y. Sekikawa, and Y. Aoki, "Optical flow estimation by matching time surface with event-based cameras," *Sensors*, vol. 21, no. 4, 2021.
- [14] A. Z. Zhu, N. Atanasov, and K. Daniilidis, "Event-based feature tracking with probabilistic data association," in *IEEE Int. Conf. Robot. Autom. (ICRA)*, 2017, pp. 4465–4470.
- [15] A. Z. Zhu, L. Yuan, K. Chaney, and K. Daniilidis, "EV-FlowNet: Self-supervised optical flow estimation for event-based cameras," in *Robotics: Science and Systems (RSS)*, 2018.
- [16] —, "Unsupervised event-based learning of optical flow, depth, and egomotion," in *IEEE Conf. Comput. Vis. Pattern Recog. (CVPR)*, 2019, pp. 989–997.
- [17] M. Gehrig, M. Millhäusler, D. Gehrig, and D. Scaramuzza, "E-RAFT: Dense optical flow from event cameras," in *Int. Conf. 3D Vision (3DV)*, 2021, pp. 197–206.
- [18] Z. Ding, R. Zhao, J. Zhang, T. Gao, R. Xiong, Z. Yu, and T. Huang, "Spatio-temporal recurrent networks for event-based optical flow estimation," *AAAI Conf. Artificial Intell.*, vol. 36, no. 1, pp. 525–533, 2022.
- [19] C. Lee, A. Kosta, A. Z. Zhu, K. Chaney, K. Daniilidis, and K. Roy, "Spike-flownet: Event-based optical flow estimation with energy-efficient hybrid neural networks," in *Eur. Conf. Comput. Vis. (ECCV)*, 2020, pp. 366–382.
- [20] Z. Teed and J. Deng, "Raft: Recurrent all-pairs field transforms for optical flow," in *European conference on computer vision*. Springer, 2020, pp. 402–419.
- [21] D. Jia, K. Wang, S. Luo, T. Liu, and Y. Liu, "Braft: Recurrent all-pairs field transforms for optical flow based on correlation blocks," *IEEE Signal Processing Letters*, vol. 28, pp. 1575–1579, 2021.
- [22] G. D'Angelo, E. Janotte, T. Schoepe, J. O'Keefe, M. B. Milde, E. Chicca, and C. Bartolozzi, "Event-based eccentric motion detection exploiting time difference encoding," *Front. Neurosci.*, vol. 14, p. 451, May 2020.
- [23] G. Orchard, R. Benosman, R. Etienne-Cummings, and N. V. Thakor, "A spiking neural network architecture for visual motion estimation," in *IEEE Biomed. Circuits Syst. Conf. (BioCAS)*, 2013, pp. 298–301.
- [24] F. Paredes-Valles, K. Y. W. Scheper, and G. C. H. E. de Croon, "Unsupervised learning of a hierarchical spiking neural network for optical flow estimation: From events to global motion perception," *IEEE Trans. Pattern Anal. Mach. Intell.*, Mar. 2019.
- [25] D. A. Clark and J. B. Demb, "Parallel computations in insect and mammalian visual motion processing," *Current Biology*, vol. 26, no. 20, pp. R1062–R1072, 2016.
- [26] B. Rueckauer and T. Delbruck, "Evaluation of event-based algorithms for optical flow with ground-truth from inertial measurement sensor," *Front. Neurosci.*, vol. 10, no. 176, 2016.
- [27] H. B. Barlow and W. R. Levick, "The mechanism of directionally selective units in rabbit's retina," *J. Physiol.*, vol. 178, no. 3, pp. 477–504, Jun. 1965.
- [28] B. Hassenstein and W. Reichardt, "Systemtheoretische analyse der zeit-, reihenfolgen- und vorzeichenbewertung bei der bewegungsperzeption des rüsselkäfers chlorophanus," *Zeitschrift für Naturforschung B*, vol. 11, no. 9–10, pp. 513–524, Oct. 1956.
- [29] J. E. Fitzgerald and D. A. Clark, "Nonlinear circuits for naturalistic visual motion estimation," *Elife*, vol. 4, p. e09123, Oct. 2015.
- [30] A. Z. Zhu, D. Thakur, T. Ozaslan, B. Pfrommer, V. Kumar, and K. Daniilidis, "The multivehicle stereo event camera dataset: An event camera dataset for 3D perception," *IEEE Robot. Autom. Lett.*, vol. 3, no. 3, pp. 2032–2039, Jul. 2018.
- [31] G. Taverni, D. P. Moeys, C. Li, C. Cavaco, V. Motsnyi, D. S. S. Bello, and T. Delbruck, "Front and back illuminated Dynamic and Active Pixel Vision Sensors comparison," *IEEE Trans. Circuits Syst. II*, vol. 65, no. 5, pp. 677–681, 2018.
- [32] E. Mueggler, H. Rebecq, G. Gallego, T. Delbruck, and D. Scaramuzza, "The event-camera dataset and simulator: Event-based data for pose estimation, visual odometry, and SLAM," *Int. J. Robot. Research*, vol. 36, no. 2, pp. 142–149, 2017.
- [33] G. Gallego and D. Scaramuzza, "Accurate angular velocity estimation with an event camera," *IEEE Robot. Autom. Lett.*, vol. 2, no. 2, pp. 632–639, 2017.
- [34] A. Z. Zhu, N. Atanasov, and K. Daniilidis, "Event-based visual inertial odometry," in *IEEE Conf. Comput. Vis. Pattern Recog. (CVPR)*, 2017, pp. 5816–5824.
- [35] C. Gu, E. Learned-Miller, D. Sheldon, G. Gallego, and P. Bideau, "The spatio-temporal Poisson point process: A simple model for the alignment of event camera data," in *Int. Conf. Comput. Vis. (ICCV)*, 2021, pp. 13 495–13 504.
- [36] E. Mueggler, G. Gallego, H. Rebecq, and D. Scaramuzza, "Continuous-time visual-inertial odometry for event cameras," *IEEE Trans. Robot.*, vol. 34, no. 6, pp. 1425–1440, Dec. 2018.
- [37] C. Brandli, R. Berner, M. Yang, S.-C. Liu, and T. Delbruck, "A 240×180 130dB 3μ s latency global shutter spatiotemporal vision sensor," *IEEE J. Solid-State Circuits*, vol. 49, no. 10, pp. 2333–2341, 2014.
- [38] F. Paredes-Valles and G. C. H. E. de Croon, "Back to event basics: Self-supervised learning of image reconstruction for event cameras via photometric constancy," in *IEEE Conf. Comput. Vis. Pattern Recog. (CVPR)*, 2021, pp. 3445–3454.
- [39] V. Brebion, J. Moreau, and F. Davoine, "Real-time optical flow for vehicular perception with low- and high-resolution event cameras," *IEEE Trans. Intell. Transportation Systems*, pp. 1–13, 2021.
- [40] T. Stoffregen, C. Scheerlinck, D. Scaramuzza, T. Drummond, N. Barnes, L. Kleeman, and R. Mahony, "Reducing the sim-to-real gap for event cameras," in *Eur. Conf. Comput. Vis. (ECCV)*, 2020, pp. 534–549.